of matching points M. The numerical results showed that using an over-determined system, i.e., $M > 2N + 1$, yields better results for the power check than obtainable with $M = 2N + 1$. However, it was also found that the least-square error becomes unacceptable (greater than 5 percent for example) if M exceeds $2N + 1$ by too large a number.

For small values of h/d or kd, both methods gave very good answers. However, when these parameters exceeded certain values, e.g., say $kd > 6\pi$ and $h/d > 0.3$ for $\theta < 45°$, the Rayleigh hypothesis failed to give acceptable results. In contrast, the analytic continuation method was found to give good results for much larger groove depths. For instance, using only one-step and two-step continuation, the case of $h/d = 0.5$ and $kd = 6\pi$ was solved with satisfactory results for $M = 18$ and $2N + 1 = 15$. The method itself is expected to give satisfactory results for even deeper grooves.

Fig. 2(a) and (b) show the variation of the power of different propagating space harmonics for a typical case of structural parameters. For this case, the Rayleigh hypothesis method fails to give even a good power check when θ exceeds 50°. Once again the analytic continuation method still gives very good results for power checks in the same range.

In conclusion, the Rayleigh hypothesis method works relatively well for the shallow gratings. One of the advantages of the method is its easier formulation and less computational effort. In contrast, the analytic continuation method, which is exact in principle, works well for much deeper gratings. It should be realized, however, that the latter requires computation time several times greater than the Rayleigh hypothesis method.

References

[1] R. F. Millar and R. H. T. Bates, "On the legitimacy of an assumption underlying the point-matching method," *IEEE Trans. Microwave Theory Tech.* (Corresp.), vol. MTT-18, pp. 325–327, June 1970.
[2] L. Lewin, "On the restricted validity of point-matching techniques," *IEEE Trans. Microwave Theory Tech.*, vol. MTT-18, pp. 1041–1047, Dec. 1970.
[3] M. L. Burrows, "Equivalence of the Rayleigh solution and the extended-boundary-condition solution for scattering problems," *Electron. Lett.*, vol. 5, pp. 277–278, June 1969.
[4] R. Mittra and D. R. Wilton, "A numerical approach to the determination of electromagnetic scattering characteristics of perfect conductors," *Proc. IEEE* (Proc. Lett.), vol. 57, pp. 2064–2065, Nov. 1969.
[5] R. Penrose, "On best approximate solutions of linear matrix equations," *Proc. Cambridge Phil. Soc.*, vol. 52, pp. 17–19, 1956.

VLF/ELF Input Impedance of an Arbitrarily Oriented Loop Antenna in a Cold Collisionless Multicomponent Magnetoplasma

THOMAS N. C. WANG AND TIMOTHY F. BELL

Abstract—**A study is made of the input impedance Z of a small strip-loop antenna with arbitrary orientation in a cold collisionless uniform multicomponent magnetoplasma. Assuming a uniform current distribution, an integral expression for Z is derived which is valid for arbitrary values of driving frequency, plasma composition and density, loop orientation angle ϕ_0, and static magnetic field strength. The integral expression is evaluated numerically for the VLF/ELF range in a plasma modeled upon the inner magnetosphere. Approximate closed-form expressions for Z are also developed. It is found that the loop VLF/ELF input reactance is essentially identical to its free space self inductance. Also the loop radiation resistance is found to be a strong function of ϕ_0 for frequencies near the lower-hybrid-resonance frequency or below the proton gyrofrequency. In addition it is found that for small loops a second-order quasi-static theory correctly predicts Z over much of the VLF/ELF range.**

Manuscript received July 12, 1971; revised October 26, 1971. This work was supported in part by NASA under Grant NGL-008 and in part by Stanford Research Institute Internal Research Funds.

T. N. C. Wang is with the Radio Physics Laboratory, Stanford Research Institute, Menlo Park, Calif. 94025.
T. F. Bell is with the Radioscience Laboratory, Stanford University, Stanford, Calif. 94305.

Introduction

The importance of studying the problem of the radiation characteristics of a loop antenna in a magnetoplasma has been made clear by a number of workers (see references in [1]). Our own motivation for continuing this study has been stated in a previous paper [1], in which we investigated the characteristics of the VLF/ELF radiation resistance of a small loop antenna embedded in a cold collisionless magnetoplasma. In [1], the orientation of the loop was assumed to be such that its axis of symmetry was parallel to the static magnetic field $\boldsymbol{B}_0$. In this paper it is our purpose to extend the analysis of [1] to the case in which the loop has an arbitrary orientation with respect to $\boldsymbol{B}_0$. Furthermore, we shall consider both the input reactance and the radiation resistance for this arbitrarily oriented loop antenna. As in [1], a full-wave solution is used.

From the results of our study, the following interesting features of the loop radiation characteristics are found.

1) Given a uniform current distribution, the VLF/ELF input reactance of a small thin strip-loop antenna in a multicomponent plasma is essentially the same as its free-space self-inductance.

2) Ion effects make the loop radiation resistance a strong function of the loop orientation angle for driving frequencies near the lower-hybrid-resonance frequency and for frequencies below the proton gyrofrequency.

3) For small loops quasi-static theory correctly predicts the loop input reactance over the entire VLF/ELF range, except in the vicinity of the electron and ion gyrofrequencies.

4) Second order quasi-static theory correctly predicts the radiation resistance of the loop whenever the loop is small and one of the characteristic electromagnetic modes of the plasma has an open refractive index surface.

II. Formulation

Consider a thin strip loop possessing a uniform time-harmonic current $I_0 e^{i\omega t}$, oriented at an arbitrary angle with respect to the magnetic field. Without losing any generality, we set the axis of symmetry of the loop in the x–z plane and let this axis make an angle ϕ_0 with respect to the z axis, which is parallel to the static magnetic field. The geometry of the problem is indicated in Fig. 1.

Using this loop as a source function in a cold uniform multicomponent magnetoplasma, the formulation developed by the authors in a previous paper [2] can be used, together with the usual relation $Z = 2P/I_0^2$ (P represents the mean complex radiated power), to determine the input impedance of the loop antenna:

$$Z = jC_0 \int_0^\infty dk \int_0^\pi \sin\theta \, d\theta \int_0^{2\pi} d\psi \, [1 + F_1 + F_2\Phi] J_1^2(V) \frac{\sin^2 U}{U^2} \quad (1)$$

where $C_0 = Z_0 \beta r^2/2\pi$, $Z_0 = 120\pi\ \Omega$, $\beta = \omega/c$, and

$$F_1 = \beta^2 \frac{k^2[\epsilon_{+1}\epsilon_{-1} \sin^2\theta + \epsilon_s\epsilon_0 \cos^2\theta] - \beta^2\epsilon_0\epsilon_{+1}\epsilon_{-1}}{\alpha(\theta)(k^2 - k_-^2)(k^2 - k_+^2)}$$

$$F_2 = \beta^2 \frac{k^2(\epsilon_s\epsilon_0 - \epsilon_{+1}\epsilon_{-1})}{\alpha(\theta)(k^2 - k_-^2)(k^2 - k_+^2)}$$

$$\Phi = \frac{\sin^2\phi_0 \sin^2\theta \sin^2\psi}{(1 - \Delta^2)}, \qquad \Delta = \sin\theta\cos\psi\sin\phi_0 + \cos\theta\cos\phi_0$$

$V = rk(1 - \Delta^2)^{1/2}$, $U = \frac{1}{2}\xi k\Delta$, $k_\pm = \beta n_\pm(\theta)$, $\alpha(\theta) = \epsilon_0 \cos^2\theta + \epsilon_s \sin^2\theta$, and where all other notation is defined in [2]–[4]. In the limit of

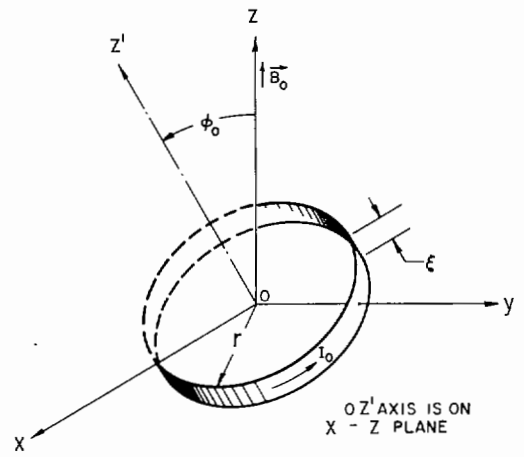

Fig. 1. Orientation of strip-loop antenna with respect to static magnetic field B_0. Loop symmetry axis lies along z' axis in body-centered coordinate system x',y',z'. y' and y axes are coincident and z' axis lies in the xz plane.

$\phi_0 \to 0$, $\Phi \to 0$, and $V \to rk \sin\theta$; (1) can then be shown to reduce identically to [1, eq. (2)].

As expressed in (1), Z is a general solution for the input impedance, valid for arbitrary values of loop orientation angle, plasma density, plasma composition, static magnetic field strength, driving frequence, and collision frequency.

III. Quasi-Static Calculations

In order to investigate the validity of quasi-static theory as applied to a loop antenna in a plasma, it is of interest to estimate the input impedance of the loop using a quasi-static approximation and then compare this with the full-wave solution. In what follows the leading terms of the quasi-static theory are calculated and it is found that in the lossless case in addition to a reactive component, a resistive component is also predicted for certain ranges of plasma parameters. As discussed in a later section, the quasi-static resistance is essentially identical to the radiation resistance as calculated by a full-wave treatment so long as the loop is sufficiently small.

A. First (Leading) Term in Quasi-Static Calculation

In the limit of $\beta \to 0$, F_1 and F_2 vanish and the integrand of (1) becomes independent of plasma parameters. In fact (1) is then identical to the quasi-static solution for the self-impedance (inductive reactance) of a uniform-current strip loop in free space, and is easily evaluated in the limit $r/\xi \gg 1$ to give the result:

$$Z^I = j\beta r Z_0 \left(\log \frac{8r}{\xi} - \frac{1}{2}\right), \qquad \frac{r}{\xi} \gg 1. \tag{2}$$

B. Second-Order Correction Term

In order to investigate (in the quasi-static limit) the effects on the loop input impedance caused by the presence of the magnetoplasma, we next consider terms of order β^2 in the integrand of (1). This second-order correction term Z^{QC} (correction to Z^I) is formally given by

$$Z^{QC} = jC_{0\epsilon_{+1}\epsilon_{-1}}\beta^2 \int_0^\infty dk \int_0^\pi d\theta \int_0^{2\pi} d\psi \cdot [1 + A\cos^2\theta + A\Phi] \frac{J_1^2(V)\sin\theta \sin^2 U}{\alpha(\theta)k^2} \frac{}{U^2} \tag{3}$$

where $A = (\epsilon_{0\epsilon_s} - \epsilon_{+1\epsilon_{-1}})/\epsilon_{+1\epsilon_{-1}}$. It is possible to show that in deriving (2) and (3) no important boundary layer terms are neglected [5].

In the limit of $\xi \to 0$, ($\xi \ll r$) the integration with respect to k can be performed straightforwardly. Furthermore the integration with respect to ψ can be carried out in terms of elliptic integrals. These two integrations yield the following expression

$$Z^{QC}(\phi_0) = jD_0 \int_0^{\pi/2} \frac{I(\theta,\phi_0)}{\alpha(\theta)} \sin\theta \, d\theta \tag{4}$$

where

$$D_0 = \frac{8(\beta r)^3}{3\pi^2} Z_{0\epsilon_{+1}\epsilon_{-1}}$$

and

$$I(\theta,\phi_0) = \sin\gamma\{[1 + A(1 + \cos^2\theta)]E(k) - A(1 - k^2)K(k) + \cos\theta\cos\phi_0(1 - A\sin^2\theta)K(k)Z(\sigma,k)\}.$$

In the preceding, $K(k)$ and $E(k)$ are the complete elliptic integrals of the first and second kinds, respectively, of modulus k; $Z(\sigma,k)$ is the Jacobian zeta function defined as $Z(\sigma,k) = E(\sigma,k) - K^{-1}(k)E(k)F(\sigma,k)$; where $F(\sigma,k)$ and $E(\sigma,k)$ are the incomplete elliptic integrals of the first and second kinds, respectively, of modulus k and argument σ; where $\gamma \equiv \phi_0$ for $\theta \le \phi_0$, while $\gamma \equiv \theta$ for $\theta \ge \phi_0$; $k \equiv \sin\theta/\sin\phi_0$ for $\theta \le \phi_0$, while $k \equiv \sin\phi_0/\sin\theta$ for $\theta \ge \phi_0$; and $\sigma \equiv \sin^{-1}(\cos\phi_0/\cos\theta)$ for $\theta \le \phi_0$, while $\sigma \equiv \sin^{-1}(\cos\theta/\cos\phi_0)$ for $\theta \ge \phi_0$.

In (4) it should be pointed out that, as a result of the relationship between k and σ, $\lim_{\theta\to\phi_0} K(k)Z(\sigma,k) \to \log[(1 + \sin\phi_0)/\cos\phi_0]$. Thus $I(\theta,\phi_0)$ is always bounded (assuming finite A) for real values of θ.

In the limit of vanishing losses, whenever $\epsilon_0/\epsilon_s > 0$, the function $\alpha(\theta)$ has no zeros on the real θ axis and Z^{QC} is entirely reactive and can be obtained directly from (4). On the other hand, when $\epsilon_0/\epsilon_s < 0$, $\alpha(\theta)$ has a zero at $\theta = \theta_r = \tan^{-1}|\epsilon_0/\epsilon_s|$ and Z^{QC} has both a resistive and a reactive part:

$$X^{QC}(\phi_0) = D_0 \int_0^{\pi/2} \frac{I(\theta,\phi_0)}{\alpha(\theta)} \sin\theta \, d\theta \tag{5a}$$

$$R^{QC}(\phi_0) = -\frac{\pi}{2} D_0 \frac{I(\theta_r,\phi_0)}{[\epsilon_s(\epsilon_s - \epsilon_0)]^{1/2}} \tag{5b}$$

where in (5a) the principal value of the integral is to be taken. It is interesting to note that in this second-order quasi-static approximation it is possible to obtain the resistive portion of Z (5b) in closed form for all values of driving frequency, plasma parameters, and loop orientation angle.

The condition $\epsilon_0/\epsilon_s < 0$, which leads to a nontrivial solution for R^{QC}, is equivalent to the condition that one of the characteristic electromagnetic modes of the plasma possesses an open refractive index surface.

For the case in which the loop symmetry axis is parallel to the static magnetic field lines ($\phi_0 = 0$) Z^{QC} can be evaluated entirely in closed form using (4) and (5). However, these solutions are not given here for the sake of brevity.

IV. Full-Wave Calculation of Input Impedance for Lossless Case

In order to case (1) into a form more suitable for numerical computations it is convenient to perform the k integration by the method of contour integration. The complexity of the contour integration can be reduced significantly if it is wished to determine Z only to lowest order in the ratio ξ/r. In this case the first term within the brackets of (1) can be integrated spearately, leading to (2), while the remainder of Z can be integrated in the limit $\xi \to 0$.

The contour integration proceeds along the lines described in [2] with the result:

$$R = Z_0(\beta r)^2\epsilon_{+1}\epsilon_{-1}\sum_{\pm}\int_0^{\pi} d\psi \int_{\theta_p} d\theta\, P_{\pm}(\theta,\psi)\, J_1^2(V_{\pm}) \tag{6a}$$

$$X^c = jZ_0(\beta r)^2\epsilon_{+1}\epsilon_{-1}\sum_{\pm}\int_0^{\pi} d\psi \cdot\left[\int_{\theta_n} P_{\pm}(\theta,\psi)\, E_{\pm}(\theta,\psi)\, d\theta - \int_{\theta_p} P_{\pm}(\theta,\psi)\, S_{\pm}(\theta,\psi)\, d\theta\right] \tag{6b}$$

where the sum is to be taken over both modes $n_{\pm}$, where the domain θ_n includes all θ $(0 \le \theta \le \pi/2)$ for which $n_{\pm}^2$ is negative, where the domain θ_p includes all θ $(0 \le \theta \le \pi/2)$ for which $n_{\pm}^2$ is positive (region of propagation in wave normal space) and where

$$P_{\pm}(\theta,\psi) = \mp\frac{[\epsilon_0 - n_{\pm}^2(1 + A\cos^2\theta + A\Phi)]}{\alpha(\theta)\,(n_+^2 - n_-^2)\,|\,n_{\pm}\,|}\sin\theta$$

$$E_{\pm}(\theta,\psi) = \frac{1}{\pi^2}\int_0^{\pi} d\alpha \int_0^{\pi} \cos 2\delta \exp\left[-2\,|\,V_{\pm}\,|\sin\alpha\sin\delta\right] d\delta$$

$$S_{\pm}(\theta,\psi) = \frac{1}{\pi^2}\int_0^{\pi} d\alpha \int_0^{\pi} \cos 2\delta \sin\left[2V_{\pm}\sin\alpha\sin\delta\right] d\alpha$$

$$V_{\pm} = \beta r n_{\pm}(1 - \Delta^2)^{1/2}.$$

Equation (6a) is a general expression for the radiation resistance R, specialized to the lossless case but valid for arbitrary value of frequency, plasma composition and density, strength of static magnetic field, and loop orientation angle. In the limit of $\phi_0 \to 0$, it can be shown that (6a) reduces identically to [1, eq. (3)]. Although approximate closed form solutions for R have been obtained from (6a) for various frequencies in the range $\omega_{He} \ge \omega \ge 0$ (ω_{He} = angular electron gyrofrequency), in the interests of brevity these solutions are not given here.

V. Numerical Results

To construct plots for the loop radiation resistance R and the reactive correction term X^c, (6a) and (6b) have been integrated numerically. In Figs. 2–5, we plot R and X^c as functions of frequency for various values of plasma density, plasma composition, static magnetic field strength, loop radius, and loop orientation angle ϕ_0.

The curves in each figure are parametric in the variables ϕ_0, r_0 and f_0/f_{He}, where $r_0 \equiv 2\pi f_{He} r/c$, f_{He} = electron gyrofrequency and f_0 = plasma frequency. The values of f_0/f_{He} used were chosen as being representative of the range of values that can be encountered in the inner magnetosphere.

Fig. 2 is a plot of R versus f/f_{He} over the range $1 \ge f/f_{He} \ge 2.5 \times 10^{-2}$. The plasma is assumed to consist of electrons and protons. The lowest frequency shown is sufficiently above the lower hybrid-resonance frequency f_{LHR} (appropriate to each value of f_0/f_{He}) so that ion effects are negligible. For any given values of f_0/f_{He} and r_0, curves plotted for parallel and perpendicular orientations lie close together and it can be shown that R is not a strong function of ϕ_0 in this frequency range. In all cases plotted, R reaches a maximum when $f \sim 0.6 - 0.8 f_{He}$. For larger values of f, R is a decreasing function of f which approaches zero rapidly as $f \to f_{He}$. When $f_0/f_{He} \le 10$ and $r_0 \le 0.1$, the curves agree with the quasi-static formula (5b) within a few percent. In this range of the parameters, R varies as r^3, and as $(f_0/f_{He})^2$. Fig. 3 is a plot of R versus f/f_{He} over the range $2 \times 10^{-3} \le f/f_{He} \le 3 \times 10^{-2}$. Only $\phi_0 = \pi/2$ is considered in this plot, since plots for $\phi_0 = 0$ are given in [1]. The plasma is assumed to consist of electrons and protons. The frequency range of this plot includes the three f_{LHR} ($f_{LHR}/f_{He} \cong 2.07 \times 10^{-2}$, 2.28×10^{-2}, and 2.33×10^{-2}) appropriate to the three normalized densities used ($f_0/f_{He} = 2$, 5, and 10). For small values of r_0, ion effects give rise to a sharp drop in the value of R as f decreases through f_{LHR}. For the larger values

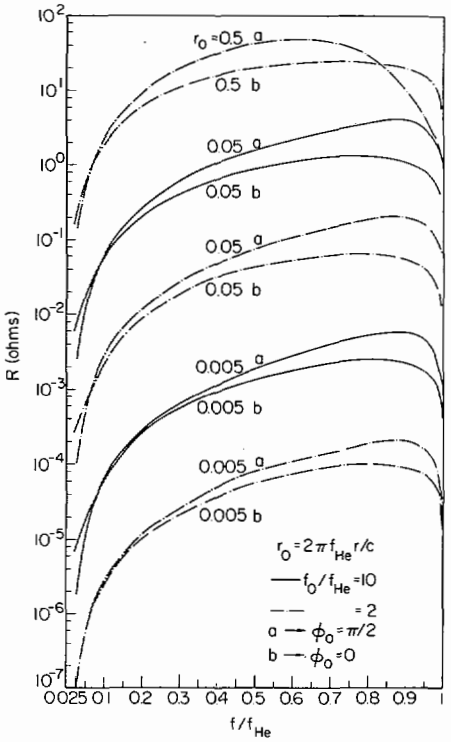

Fig. 2. Loop radiation resistance as function of normalized frequency f/f_{He} for various values of normalized radius r_0 and density ratio f_0/f_{He}. Two orientation angles are considered, $\phi_0 = 0$ and $\pi/2$.

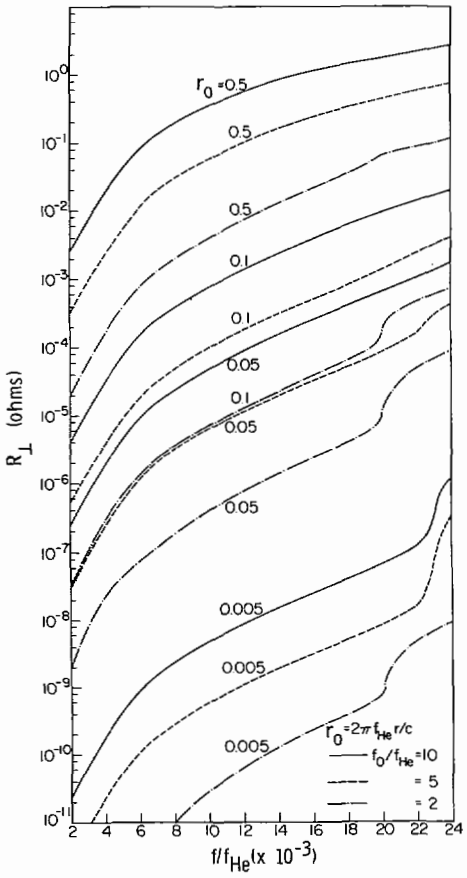

Fig. 3. Loop radiation resistance as function of normalized frequency f/f_{He} for various values of normalized radius r_0 and density ratio f_0/f_{He}. Orientation angle is $\phi_0 = \pi/2$.

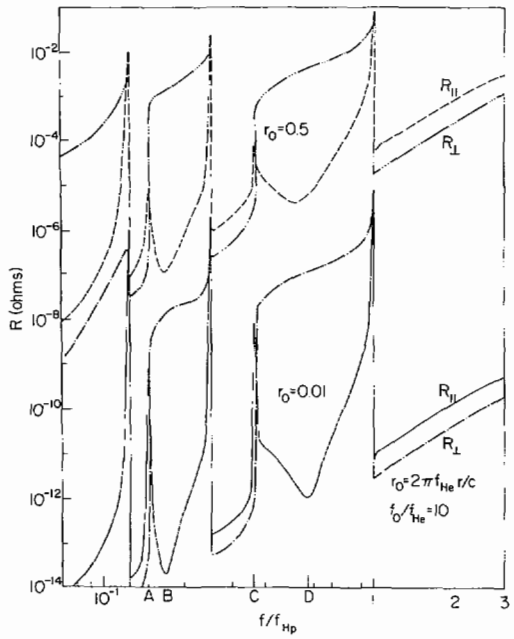

Fig. 4. Loop radiation resistance as function of normalized frequency f/f_{Hp} and normalized radius r_0 in multiion magnetoplasma. Four species plasma is assumed, electrons, protons (70 percent), He^+(20 percent) and O^+(10 percent). Two orientation angles are considered $\phi_0 = 0$ ($R_{||}$) and $\phi_0 = \pi/2$ ($R_\perp$). Density ratio is assumed to be 10.

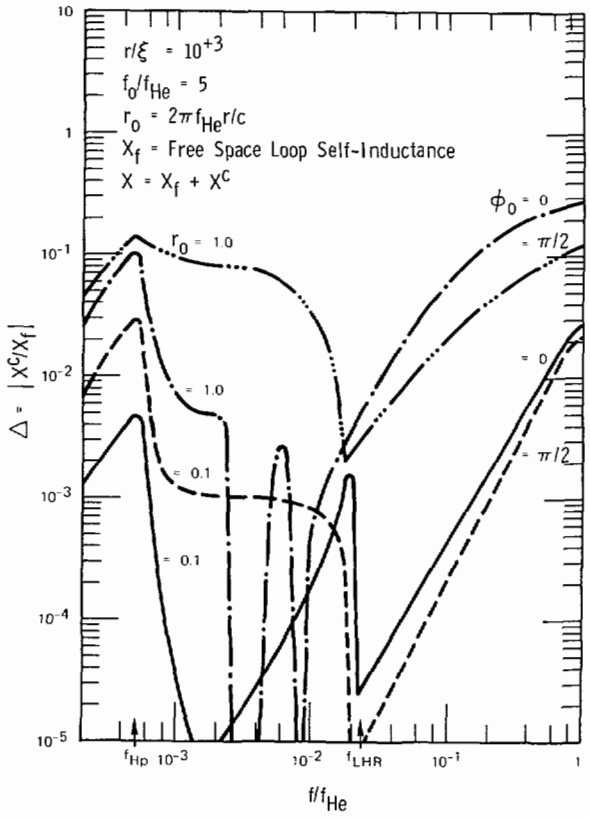

Fig. 5. Loop reactance correction term X_c, normalized to free space loop self-inductance X_f and plotted as function of normalized frequency f/f_{He} and normalized radius r_0 for two values of orientation angle $\phi_0 = 0$ and $\pi/2$. Ratio of loop radius to height ξ is assumed to be 10^3 and density ratio f_0/f_{He} is assumed to be 5.

of r_0, however, this sharp dropoff tends to disappear. A comparison of Fig. 3 with [1, fig. 2] shows that for small r_0, R is a strong function of ϕ_0 near f_{LHR}, $R(\phi_0 = 0)$ being orders of magnitude larger than $R(\phi_0 = \pi/2)$. For $f < f_{LHR}$, $R(\phi_0)$ decreases monotonically as f decreases, with $R_\perp \sim 4R_{||}$ for $f \ll f_{LHR}$.

Fig. 4 shows a plot of R versus f/f_{Hp} over the range $7 \times 10^{-2} \leq f/f_{Hp} \leq 1$ (f_{Hp} = proton gyrofrequency). Two sets of curves are plotted, one for $r_0 = 0.5$ and one for $r_0 = 0.01$; and in each set two values of orientation angle are considered, $\phi_0 = 0$ and $\pi/2$. In all cases it is assumed that $f_0/f_{He} = 10$. The plasma is assumed to consist of electrons and three ions: atomic hydrogen, atomic helium, and atomic oxygen. The composition of the plasma is assumed to be 70 percent H^+, 20 percent He^+, and 10 percent O^{++}.

The effects on R due to the presence of multiple ions are clearly visible in the curve sets of Fig. 4, and it is interesting to see the dramatic changes in R that can be produced by a variation of orientation angle.

In each set both $R_\perp$ and $R_{||}$ show relative maxima slightly below the ion gyroresonance frequencies and relative minima slightly above the ion gyrofrequencies but at other frequencies their behavior can be completely different. For instance at the multiple-ion hybrid-resonance frequencies (points labeled A and D on the frequency axis, see [1] for definition), $R_{||}$ has a sharp maximum while $R_\perp$ exhibits a sharp decrease in value. Furthermore near the crossover frequencies (points labeled B and D on the frequency axis, see [1] for definition), $R_{||}$ has a minimum while $R_\perp$ has a relatively high value. The difference between $R_{||}$ and $R_\perp$, although many orders of magnitude at small values of r_0, tend to decrease for larger values of r_0. Fig. 5 is a plot of the loop reactance correction term X^c, normalized to the free-space loop self-inductance X_f and plotted as a function of f for two values of r_0 and two values of ϕ_0. It is assumed that $f_0/f_{He} = 5$, $r/\xi = 10^3$, and that the plasma consists of protons and electrons. In preparing Fig. 5, X^c was calculated from (6b) while X_f was calculated from (2). Thus $X_f + X^c$ represents the complete full-wave loop reactance and the ratio $\Delta = |X^c/X_f|$ represents the fractional variation in the loop reactance due to the presence of the plasma. Although Δ varies widely as a function of r_0 and ϕ_0, it is never larger than approximately 0.3 when $r_0 \leq 1$. It can be shown that Δ is a monotonically increasing function of r_0 and thus in principle Δ could be increased beyond the values shown in Fig. 5 by specifying a larger value of r_0. On the other hand, Fig. 5 is plotted under the assumption that the loop possesses a uniform current distribution. This assumption appears reasonable at any given f so long as the loop is small compared to the maximum wavelength λ_m of the medium at that f. However for $r_0 \geq 1$, it can be shown that the loop circumference exceeds λ_m over most of the frequency range of Fig. 5. Consequently values of Δ for $r_0 > 1$ were not considered as being meaningful and were not plotted.

It can be shown that for the smaller value of r_0 in Fig. 5, the values of Δ obtained from the full-wave solution generally agree to within a few percent with the quantity $\Delta^{QC} \equiv |X^{QC}/X_f|$, where X^{QC} is obtained from (5a). Large discrepancies between Δ and Δ^{QC} arise only near the electron and proton gyrofrequencies. Thus it is evident that for small loops, the second order quasi-static theory will predict the input reactance over almost the entire VLF/ELF range.

VI. Discussion and Conclusions

The calculations shown in Fig. 5 indicate that the VLF/ELF input reactance of a thin strip-loop antenna ($r/\xi \gg 1$) in a cold multicomponent magnetoplasma is essentially the same as the input reactance of this same loop in free space. This result is supported by the recent experimental work of Duff and Mittra [6] in which the (small signal) input impedance of a small loop in a magnetoplasma was found to have only a second order dependence on the plasma. From this experiment it can be inferred that the loop does not couple strongly to the plasma through ion sheath effects. Although this finding enhances the usefulness of the present

theory, a word of caution is necessary. As $f \to f_{He}$ or $f \to f_{Hp}$ the maximum wavelength of the major radiating mode will eventually become smaller than the loop radius, and when this occurs it becomes extremely doubtful that the loop current can remain uniform. As the current becomes nonuniform the loop will develop an electric dipole moment and will begin to couple more strongly to the plasma through the ion sheath. Consequently, there is good reason to believe that the loop reactance will vary markedly from its free space value at both f_{He} and f_{Hp} (and in all other cases where the loop current distribution is reasonably nonuniform).

Duff and Mittra [6] have also investigated the input impedance Z of a small loop in a magnetoplasma from the theoretical point of view. Two theories were used: an approximate quasi-static theory and a theory based on a uniaxial approximation. A comparison of the approximate expressions for Re Z developed by Duff and Mittra with our own results shows a significant difference over most of the VLF/ELF range. We infer that their approximate theories lack sufficient accuracy to allow a meaningful evaluation of the VLF/ELF radiation resistance.

One of the most interesting results of our work is the fact that the second order quasi-static theory can be used to accurately predict both the real and imaginary portions of the input impedance of a small loop in a multicomponent plasma. This result tends to encourage the idea that the difficult problem of calculating the input impedance of a loop antenna with both nonuniform current distribution and ion sheath might be successfully attacked using quasi-static theory.

Acknowledgment

The authors gratefully acknowledge the support and encouragement of Professor R. A. Helliwell and the Radioscience Laboratory Staff during the course of this research.

References

[1] T. F. Bell and T. N. C. Wang, "Radiation resistance of a small filamentary loop antenna in a cold multicomponent magnetoplasma," *IEEE Trans. Antennas Propagat.*, vol. 19, pp. 517–522, July 1971.
[2] T. N. C. Wang and T. F. Bell, "Radiation resistance of a short dipole immersed in a cold magnetoionic medium," *Radio Sci.*, vol. 4, pp. 167–177, Feb. 1969.
[3] ——, "On VLF radiation resistance of an electric dipole in a cold magnetoplasma," *Radio Sci.*, vol. 5, pp. 605–610, Mar. 1970.
[4] ——, "On VLF radiation fields along the static magnetic field from sources immersed in a magnetoplasma," *IEEE Trans. Antennas Propagat.* (Commun.), vol. AP-17, pp. 824–827, Nov. 1969.
[5] R. L. Fante, "On the admittance of the infinite cylindrical antenna," *Radio Sci.*, vol. 1, pp. 1041–1044, Sept. 1966.
[6] G. L. Duff and R. Mittra, "Loop impedance in magnetoplasma: theory and experiment," *Radio Sci.*, vol. 5, pp. 81–94, Jan. 1970.

Reflection and Transmission of Electromagnetic Waves Obliquely Incident upon a Moving Compressible Plasma Slab

TOSHITAKA KOJIMA, TSUNEHITO HIGASHI, AND KIYOYASU ITAKURA

***Abstract*—Reflection and transmission of electromagnetic waves by a moving compressible plasma slab is treated. Power reflection and transmission coefficients are obtained and the numerical results of the power reflection coefficient are presented for both the cases of cold plasma slab and compressible plasma slab.**

Introduction

With recent progress of the space exploration, electromagnetic field problems in a moving medium have been theoretically and widely studied by Tai [1], [3], Lee and Papas [2], and others [4]–[9]. Reflection and transmission problems by a moving bounded medium such as a dielectric or a plasma slab, have been studied by Yeh and Casey [4], Yeh [5],[6], Kong and Cheng [7], and Chawla and Unz [8]. However, the reflection and transmission of electromagnetic waves by a moving compressible plasma slab has not yet been treated. In this communication, we discuss the reflection and transmission of electromagnetic waves by a compressible plasma slab moving parallel to the plane of incidence and the slab boundaries, for a case where a plane electromagnetic wave with its magnetic field vector polarized normal to the plane of incidence is obliquely incident upon the slab. The power reflection and transmission coefficients are obtained and the effects of the motion of the slab on the power reflection coefficient are discussed by showing some numerical results of it and comparing the result with the case of a moving cold plasma slab.

Manuscript received July 13, 1971; revised October 18, 1971.
The authors are with the Department of Electrical and Communication Engineering, Faculty of Engineering, Osaka University, Suita, Osaka, Japan 565.

Reflection and Transmission Coefficients

In a rectangular coordinate system (x,y,z), we assume that a compressible plasma slab $(0 > z > -d)$ is moving with a constant velocity v parallel to the x axis in free space $(z > 0,\ z < -d)$. Let us consider a case where a plane electromagnetic wave in the region $z > 0$ with its magnetic field vector polarized in y–z plane, is obliquely incident upon the slab. In the laboratory frame, the incident wave is represented by

$$H_{iy} = H_0 \exp\left[i(k_{ix}x - k_{iz}z - \omega t)\right]$$

$$E_{iz} = -\frac{k_{iz}}{\epsilon_0 \omega} H_{iy}, \qquad z > 0 \tag{1}$$

where

$$k_{ix} = k_0 \sin\theta_i, \qquad k_{iz} = k_0 \cos\theta_i, \qquad k_0 = \frac{\omega}{c} \tag{2}$$

and H_0 is the amplitude of the incident wave, ϵ_0 the permittivity of free space, θ_i the angle of incidence, and c the light velocity in free space, respectively.

Applying the Lorentz transformation [13] for field vector and wave-four vectors to (1) and (2), the problem considered here results in the boundary value problem for a stationary compressible plasma slab. Since the reflection and transmission problems by a stationary compressible plasma medium have been analyzed [10], [11], we can easily obtain the reflected and the transmitted waves in the rest frame of the moving slab. With the aid of the Lorentz transformation, the reflected and transmitted waves obtained in the rest frame of the slab are transformed into the one in the laboratory frame, as follows.

For reflected wave

$$H_{ry} = H_r \exp\left[i(k_{rx}x + k_{rz}z - \omega t)\right]$$

$$E_{rz} = \frac{k_{rz}}{\epsilon_0 \omega} H_{ry}, \qquad z > 0. \tag{3}$$

For transmitted wave

$$H_{ty} = H_t \exp\left[i(k_{tx}x - k_{tz}z - \omega t)\right]$$

$$E_{tz} = -\frac{k_{tz}}{\epsilon_0 \omega} H_{ty}, \qquad z < -d \tag{4}$$

where

$$H_r = \frac{f}{a + ib} \cdot H_0 \tag{5a}$$

$$H_t = \frac{g}{a + ib} \cdot H_0 \exp\left(-ik_{iz}'d\right) \tag{5b}$$

$$k_{rx} = k_{tx} = k_{ix}, \qquad k_{rz} = k_{tz} = k_{iz} \tag{5c}$$